Evaporation and fission of the primary fragments produced by multinucleon transfer reactions

P. W. Wen,[1,2] C. J. Lin,[1,3,*] C. Li,[4] L. Zhu,[5] F. Zhang,[6] F. S. Zhang,[4,7,8] H. M. Jia,[1] F. Yang,[1] N. R. Ma,[1] L. J. Sun,[1,9] D. X. Wang,[1] F. P. Zhong,[1,3] H. H. Sun,[1] L. Yang,[1,10] and X. X. Xu[1,11]

[1]*China Institute of Atomic Energy, Beijing 102413, China*

[2]*Bogoliubov Laboratory of Theoretical Physics, Joint Institute for Nuclear Research, 141980 Dubna, Russia*

[3]*Department of Physics, Guangxi Normal University, Guilin 541004, China*

[4]*Beijing Radiation Center, Beijing 100875, China*

[5]*Sino-French Institute of Nuclear Engineering and Technology, Sun Yat-sen University, Zhuhai 519082, China*

[6]*Department of Electronic Information and Physics, Changzhi University, Changzhi 046011, China*

[7]*Key Laboratory of Beam Technology of Ministry of Education, College of Nuclear Science and Technology, Beijing Normal University, 100875 Beijing, China*

[8]*Center of Theoretical Nuclear Physics, National Laboratory of Heavy Ion Accelerator of Lanzhou, 730000 Lanzhou, China*

[9]*School of Physics and Astronomy, Shanghai Jiao Tong University, Shanghai 200240, China*

[10]*Center for Nuclear Study, University of Tokyo, RIKEN campus, 2-1 Hirosawa, Wako, Saitama 351-0198, Japan*

[11]*Department of Physics, The University of Hong Kong, Hong Kong, China*

(Received 20 August 2018; revised manuscript received 18 December 2018; published 7 March 2019)

The multinucleon transfer (MNT) reaction has aroused wide interest in recent years largely due to its ability to produce neutron-rich heavy nuclei. The semiclassical model GRAZING can describe well the experimental MNT data for many medium-heavy systems, but only simply considers neutron evaporation in the deexcitation of primary fragments. In order to describe the final MNT products for heavy and even superheavy systems, we try to consider both the transfer and subsequent deexcitation processes by combining, for the first time, the GRAZING model and the statistical-decay model GEMINI as well as the improved version GEMINI++. Considering fission in the deexcitation of primary fragments by GEMINI++ model, the isotope distributions of final fragments are much wider than those only by GRAZING model, indicating an important role of fission in the deexcitation process for heavy and superheavy fragments. However, our results have large deviations from the GRAZING-F results, which may result from the different technique adopted in the deexcitation process. Moreover, it is shown that the GEMINI++ model is more reasonable than the GEMINI model, because the latter overpredicts the fission probability and the width of fission isotope distributions to a large extent. With GEMINI++ model, the predictions of cross sections for final isotopes can be improved by taking into account charged-particle evaporations, especially the α evaporation.

DOI: 10.1103/PhysRevC.99.034606

I. INTRODUCTION

The complicated multinucleon transfer (MNT) reactions, which include quasielastic transfer, deep inelastic transfer, and part of the quasifission process [1–3], have aroused wide interest [2] in the last two decades. Both theoretical predictions and experimental hints suggest that MNT process is a substantial approach to produce neutron-rich isotopes of heavy nuclei [2,4–10]. It is the only promising way known at present to produce neutron-rich superheavy nuclei, because the fragmentation reaction is not applicable due to the lack of target or projectile heavy enough, and meanwhile fusion reaction only can produce neutron-deficient heavy nuclei. Recently, many MNT experiments have been performed aimed at producing new isotopes [11–17]. For instance, five new neutron-deficient isotopes were discovered in the MNT reaction of ^{48}Ca + ^{248}Cm at GSI [18]. But no new neutron-rich superheavy nuclei were discovered yet, owing to the extremely low production cross section and identification efficiency.

The cross sections of final neutron-rich superheavy isotopes are usually extremely low. Therefore, systematic studies on the optimum projectile-target combinations and incident energies will provide important information on the production of superheavy nuclei by MNT reactions, which is a substantial challenge both experimentally and theoretically. Moreover, the pair and/or cluster transfers may play an important role in the MNT process [2], but the current knowledge is still limited.

Different theoretical models have been developed to describe the MNT process under certain approximations, such as the GRAZING model [2,19,20], the CWKB model [21,22], the dinuclear system (DNS) model [5,8,9,23–28], the Langevin equations [7,29,30], the time-dependent Hartree-Fock (TDHF) model [31–35], and the quantum molecular dynamics (QMD) model [36–38]. These models give us information about the production of the primary fragments in MNT reactions. Afterwards, statistical decay models have to be used

*Corresponding author: cjlin@ciae.ac.cn

to consider the deexcitaion processes to get the distribution of the final fragments.

The GRAZING model was proposed by Winther *et al.* [19,20,39–41] to describe the grazing reactions of heavy ions, where quasielastic and deep inelastic processes are treated simultaneously by considering the deep inelastic reaction as a part of grazing collisions. By combining the classical trajectory and quantum penetration or transition probability, different type of reactions can be well described, including capture, transfer, or inelastic excitation [2,40,42]. The predictions for MNT reactions by GRAZING are often used as a reference for the experimental study, such as ^{58}Ni + ^{124}Sn [42], ^{58}Ni + ^{208}Pb [43], ^{136}Xe + ^{208}Pb [15], ^{136}Xe + ^{198}Pt [14], and ^{136}Xe + ^{238}U [44].

Despite the excellent descriptions for few nucleon transfer reactions [2,42], there are three limitations for GRAZING. First, the transfer of many nucleons in the model is treated in a successive way and pair or cluster transfers are not considered. While the pairing effect included in the CWKB model has been demonstrated to have a significant influence [21,22,45,46]. Second, the GRAZING model describes the transfer reaction at the scattering process, when capture does not happen yet. It was suggested that dinuclear evolution can be used as a natural connection of the GRAZING model for future theoretical developments, in order to obtain an overall description of heavy-ion reactions [20]. The first attempt to combine GRAZING with DNS was achieved in Ref. [47]. As a result, the description of experimental MNT cross sections is improved to a large extent. Another limitation is that only the simple neutron evaporation is incorporated, while fission in the deexcitation of primary heavy fragments is not considered. For improving this, the fission of primary fragments generated in MNT reactions has been included in the GRAZING-F model [48] and the productions of new neutron-rich actinide isotopes were predicted [49], where the competition between neutron emission and fission is simulated by the classical formalism of Vandenbosch and Huizenga [50].

The influence of neutron and charged particle evaporation in the MNT reaction of heavy systems has not been well studied yet. Besides, it is necessary to test the fission of primary fragments generated by GRAZING with more systematically testified models, for instance, the Monte Carlo statistical-model code GEMINI [35,38,51–54] and the improved version GEMINI++ [32–35,55,56]. In this paper, the evaporation and fission of the MNT primary fragments are studied by using the semiclassical model GRAZING accompanied by GEMINI and GEMINI++. We will show that the results of the GRAZING model accompanied by different deexcitation models are quite different from each other, and also from the GRAZING-F results in Ref. [49].

The arrangement of this paper is as follows. Theoretical frameworks of GRAZING, GEMINI and GEMINI++ models are outlined in Sec. II. The MNT products for the different systems are calculated to examine the transfer cross sections predicted by GRAZING plus different deexcitation models in Sec. III, together with some discussions. Finally, conclusions are presented in Sec. IV.

II. THEORETICAL FRAMEWORK

The GRAZING model is able to predict the reaction products in the multinucleon transfers that occur in the grazing region, where the distance between the two colliding heavy nuclei is (near but) larger than the sum of their half-density radii [19,20,40,41,57]. It was assumed that the transfer probability between two given states is much smaller than unity in the grazing region. The characteristic function is engaged to treat transfer and inelastic channels simultaneously instead of directly solving the coupled equations.

In the GRAZING model, the probability distribution in excitation energy $E^\star$, transferred neutron number $\tilde{N}$, and proton number $\tilde{Z}$, and angular momentum M is given by

$$\begin{aligned} P(E_{\rm a}^\star, E_{\rm A}^\star, M_{\rm a}, M_{\rm A}, \tilde{N}, \tilde{Z}) &= \langle\bar{\Psi}(t)|\delta(E_{\rm a}^\star - \hat{H}_{\rm a})\delta(E_{\rm A}^\star - \hat{H}_{\rm A})\delta(M_{\rm a} - \hat{M}_{\rm a})\delta(M_{\rm A} - \hat{M}_{\rm A})\delta(\tilde{N} - \hat{N})\delta(\tilde{Z} - \hat{Z})|\Psi(t)\rangle \\ &= \frac{1}{(2\pi)^6}\int_{-\infty}^{\infty} d\beta_{\rm a} d\beta_{\rm A} d\zeta_{\rm a} d\zeta_{\rm A} d\gamma_{\rm N} d\gamma_{\rm Z} Z(\beta_{\rm a}, \beta_{\rm A}, \zeta_{\rm a}, \zeta_{\rm A}, \gamma_{\rm N}, \gamma_{\rm Z}) \\ &\quad \times \exp[-i\tilde{N}\gamma_{\rm N} - i\tilde{Z}\gamma_{\rm Z} - iM_{\rm a}\zeta_{\rm a} - iM_{\rm A}\zeta_{\rm A} - iE_{\rm a}^\star\beta_{\rm a} - iE_{\rm A}^\star\beta_{\rm A}], \end{aligned} \tag{1}$$

where γ, β and ζ are the Fourier transform parameters for the corresponding nucleon number, angular momentum, and excitation energy. The characteristic function in the above formula is

$$Z(\beta_{\rm a}, \beta_{\rm A}, \zeta_{\rm a}, \zeta_{\rm A}, \gamma_{\rm N}, \gamma_{\rm Z}) = \langle\bar{\Psi}(t)|\exp[i\hat{H}_{\rm a}\beta_{\rm a} + i\hat{H}_{\rm A}\beta_{\rm A} + i\hat{M}_{\rm a}\zeta_{\rm a} + i\hat{M}_{\rm A}\zeta_{\rm A} + i\hat{N}\gamma_{\rm N} + i\hat{Z}\gamma_{\rm Z}]|\Psi(t)\rangle, \tag{2}$$

where

$$\begin{aligned} \hat{H}_{\rm a} &= \sum_{i\in\nu,\pi}\epsilon_{a_i'}a^\dagger(a_i')a(a_i) + \sum_{n'}\hbar\omega_{n'}a^\dagger(n')a(n'), \quad \hat{H}_{\rm A} = \sum_{i\in\nu,\pi}\epsilon_{a_i}a^\dagger(a_i)a(a_i) + \sum_{n}\hbar\omega_{n}a^\dagger(n)a(n), \\ \hat{M}_{\rm a} &= \sum_{i\in\nu,\pi}m_i'a^\dagger(a_i')a(a_i) + \sum_{n'}\mu_{n'}a^\dagger(n')a(n'), \quad \hat{M}_{\rm A} = \sum_{i\in\nu,\pi}m_ia^\dagger(a_i)a(a_i) + \sum_{n}\mu_{n}a^\dagger(n)a(n), \\ \hat{N} &= \sum_{i\in\nu}a^\dagger(a_i')a(a_i), \quad \hat{Z} = \sum_{i\in\pi}a^\dagger(a_i)a(a_i). \end{aligned} \tag{3}$$

In the above formulas, a_i, ϵ_{a_i}, and m_i are the single-particle quantum number, energy and the magnetic quantum number of the target, while a'_i, $\epsilon_{a'_i}$, and m'_i are those of the projectile. The quantum numbers of collective modes in the target and projectile are represented by n and n'. The state vector $|\Psi(t)\rangle$ and its adjoint $\langle\bar{\Psi}(t)|$ are the solutions of the semiclassical coupled equations in the prior and post representations, respectively, which govern the exchange of nucleons in the mean-field approximation [57,58].

The state vector in prior representation can be written as

$$|\Psi(t)\rangle = \mathcal{T}\exp\Big[-\frac{i}{\hbar}\int_{-\infty}^{t}\bar{V}(t')dt'\Big]|0\rangle, \tag{4}$$

where $\mathcal{T}$ is the time-ordering operator. The interaction $\bar{V}(t)$ is expressed in the interaction representation and contains the contributions from both transfer and inelastic channels, which are taken into account by using the parameterized form factors [59,60]. The harmonic approximation is adopted to treat collective vibrations, and the average single-particle level densities are introduced to deal with the transfer processes. After substituting the state vector in Eq. (3) into Eq. (2), an analytical form of the characteristic function can be obtained by keeping the first two orders of the time-order operator in Eq. (4). More details of the derivations can be seen in the Appendix of Ref. [19]. The particles between two nuclei are exchanged under the mean-field approximation. Therefore, the results will become unreliable when the masses of colliding nucleus are too small. Because the single-particle transfer form factor used in the GRAZING model is obtained at low energy, it requires that the bombarding energy cannot be too high, typically less than 10 MeV/nucleon in the laboratory system [59,60].

With the characteristic function, it is able to calculate the correlated probabilities in energy excitation, transfer of nucleons, and angular momentum distribution. The total energy distribution for an intermediate configuration (a, A) can be obtained directly from Eq. (1) by leaving out other variables, i.e.,

$$P(E_a^\star, E_A^\star) = \frac{1}{(2\pi)^2}\int_{-\infty}^{\infty} d\beta_a d\beta_A Z(\beta_a, \beta_A, 0, 0, 0, 0) \times \exp[-iE_a^\star\beta_a - iE_A^\star\beta_A]. \tag{5}$$

Since the assumption of the energy-independent level density, the energy distributions of the two reactants are identical. After some transformations, the above formula can be written in a more compact way. It is demonstrated that the energy distribution is similar to the Gamma-distribution [19]. Therefore, the excitation energy distribution is taken as the Gamma-distribution for the original neutron evaporations in the GRAZING model.

The capture probability $P_{\rm cap}$ defines the boundary between grazing inelastic collision and capture process [20,40]. The relative motion of the two colliding nuclei is governed by the classical equation by taking into account the effect of surface deformation, namely

$$m_{\rm aA}\ddot{S} = \frac{l^2}{m_{\rm aA}r^3} + \frac{Z_aZ_Ae^2}{r^2} - (1+\kappa)\frac{\partial U_{aA}}{\partial r}, \tag{6}$$

where l is the orbital angular momentum, $m_{\rm aA}$ is the reduced mass, and κ is the factor that determines the change of force due to the surface collective modes [20,42]. The surface distance is expressed as $S = r - R_a - R_A$, where r is the relative distance between the projectile and the target, R_a and R_A refer to the radii of the projectile and the target. At the turning point where $\dot{S} = 0$, large deformation will occur and the system will merge to form a compound nucleus if $\ddot{S} < 0$. The capture probability $P_{\rm cap}$ is calculated by considering the impact of surface modes and transfer, as well as the effect of quantum penetration at the capture distance [20,42], which can be obtained by solving Eq. (6).

Similar to deducing Eq. (5), the transfer probability $P_{\rm tr}(Z, A, E)$ can be obtained by leaving out other variables in Eq. (1). The total transfer cross section can be expressed as a sum of the partial waves with orbital angular momentum l,

$$\sigma_{\rm tr}(Z, A, E) = \frac{\pi\hbar^2}{2m_{\rm aA}E}\sum_l(2l+1) \times [1 - P_{\rm cap}(E, l)]P_{\rm tr}(Z, A, E). \tag{7}$$

The nuclear potential used in GRAZING is the Woods-Saxon type with parameters derived from Akyüz-Winther parametrization [19,20,61], which was obtained by fitting large scale of experimental scattering data and has been successfully used in describing different kinds of reactions in the grazing region,

$$U_{aA} = -16\pi\gamma' a\frac{R_aR_A}{R_a+R_A}\frac{1}{1+\exp[(r-R_a-R_A)/a]}, \tag{8}$$

where

$$\frac{1}{a} = 1.17\big[1 + 0.53\big(A_a^{-1/3} + A_A^{-1/3}\big)\big] \tag{9}$$

$$R_i = 1.2A_i^{1/3} - 0.09 \tag{10}$$

$$\gamma' = 0.95\Big[1 - 1.8\frac{(N_a - Z_a)(N_A - Z_A)}{A_aA_A}\Big]. \tag{11}$$

A_i, Z_i, and N_i in above formulas are the mass, proton, and neutron numbers of the nucleus i, respectively.

In this work, GEMINI and GEMINI++ will be linked to GRAZING, respectively, to deal with the deexcitation of the fragments. To do so, the neutron evaporation included in GRAZING has to be switched off to avoid the double counting. GEMINI was originally proposed [62] by Charity aimed at predicting the complex-fragment emission in fusion reactions. The improved version GEMINI++ [55,56] predicts the fission of heavy nuclei better. The main difference between GEMINI++, GEMINI, and most other statistical decay models is that they can take into account not only light particle evaporation and symmetric fission, but also all possible binary-decay modes [62]. The decay of heavy fragments will undergo a series of sequential binary decays until they are not allowed due to energy conservation or improbable due to the γ-ray competition. In GEMINI and GEMINI++ [55,56,63,64], evaporation of nucleons and light particles is predicted by the Hauser-Feshbach formalism. The Moretto's generalized transition-state formalism [65] is adopted to deal with the decay of lighter compound nuclei and asymmetry

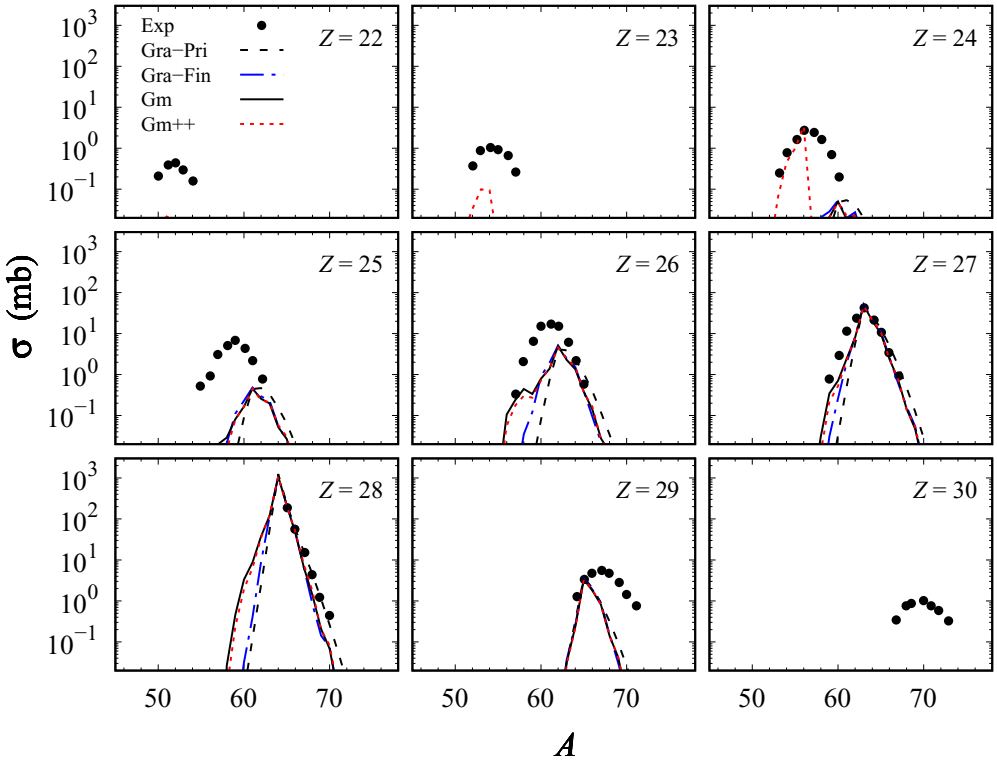

FIG. 1. Projectilelike isotopic production cross sections for ^{64}Ni + ^{238}U at $E_{\text{c.m.}} = 307.5$ MeV. The experimental data from Ref. [68] are shown as solid circles. The dashed (Gra-Pri) and dash-dotted lines (Gra-Fin) represent the primary fragments and final fragments generated by the original GRAZING model. Final fragments produced by GRAZING complemented with GEMINI and GEMINI++ are represented by solid (Gm) and the dotted lines (Gm++), respectively.

decay of heavier compound nuclei. An important improvement of GEMINI++ compared to GEMINI is the fission for more heavier systems is described by the Bohr-Wheeler formalism by considering the structure evolution [66], with the width of the mass distributions of the fission fragments obtained from systematics [67].

III. RESULTS AND DISCUSSIONS

The default parameters of GRAZING, GEMINI, and GEMINI++ are adopted in the present work. Because the fragments created by GRAZING are from direct reaction, very few nucleons are transferred compared to the projectile and target. Hence, the angular momentum transferred to the primary products is assumed to be zero in the calculations, which is the same as in Ref. [49]. In GEMINI or GEMINI++ calculations, 5000 events are simulated for each primary fragment at a certain excitation energy and angular momentum.

A. Evaporation of light particles

The evaporations of charged particles, such as p, d, t, ^{3}He, α, and $^{6-8}$Li, are taken into account in GEMINI and GEMINI++, respectively. The MNT reaction for ^{64}Ni + ^{238}U at $E_{\text{c.m.}} = 307.5$ MeV is taken as an example here. Figure 1 displays the isotopic production cross sections, where the experimental data shown as solid circles are obtained from Ref. [68]. The cross sections for primary and final fragments predicted by GRAZING, as well as those predicted by GRAZING complemented with GEMINI and GEMINI++, are represented by different lines in the figure.

It can be seen that the cross sections for final fragments denoted by the dash-dotted line are shifted to the relative neutron-deficient side by considering simple neutron evaporation. This is clear for the cases of $Z = 25, 26, 27$ but not so obvious for other cases. The cross sections for final fragments predicted by incorporating GEMINI and GEMINI++ are usually shifted to more neutron-deficient side. In the cases of $Z = 26, 27, 28$, more neutrons are evaporated distinctly by incorporating GEMINI and GEMINI++ and the predictions are similar for the two cases. The isotopic distributions are both wider than the original one. It will have a larger influence on the predictions of neutron-deficient nuclei, which have not been detected yet. Taking the isotope with $Z = 28$ and $A = 60$ as an example, the cross sections for primary and final fragments predicted by GRAZING are 0.0058 mb and 0.032 mb, respectively. But the predictions by incorporating GEMINI++ and GEMINI are 1.94 mb and 3.31 mb, which are about two orders higher than the original one.

In Fig. 2, the cross sections with respect to neutron number are plotted. The advantage of this kind of plot is to eliminate the effect of pure proton evaporation. Proton evaporation plays an important role in the charged particle evaporation in GEMINI and GEMINI++. If only protons are evaporated, the distribution will not be changed. Therefore, it is easier to clarify the role of neutron evaporation by the plot. In the

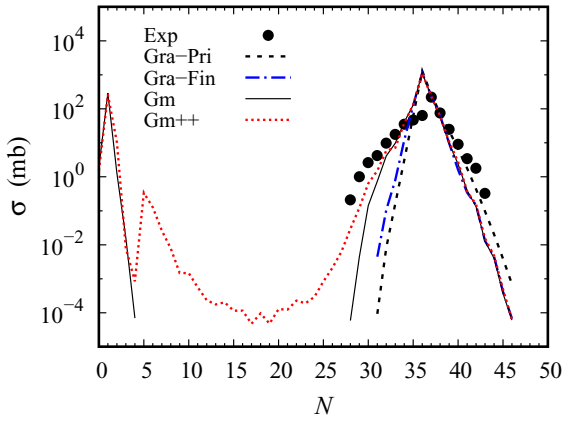

FIG. 2. Same as Fig. 1 but for the distribution with neutron number.

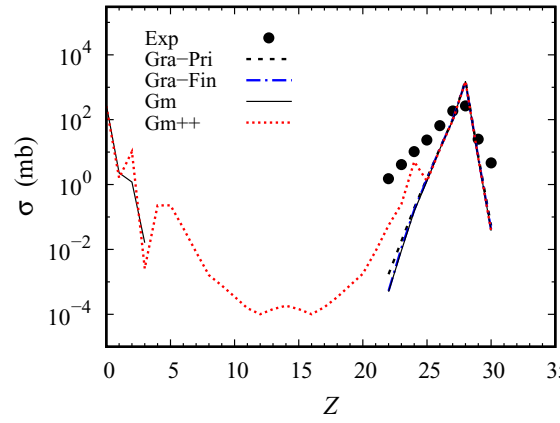

FIG. 3. Same as Fig. 1 but for the distribution with proton number. The dash-dotted and the solid lines almost overlap for $Z = 22$–30.

figure, the dash-dotted line predicted by the original neutron evaporation method is very close to the dashed line, i.e., the distribution of primary fragments. Predictions considering GEMINI and GEMINI++ are much wider than the original GRAZING. The predictions with GEMINI++ are closest to the experimental values, but still narrower than the experimental ones. Other reaction mechanisms such as quasifission, which may play a role here [68] should be studied further.

The large peaks of proton and neutron, namely $N = 0$ and $N = 1$, can be seen in Fig. 2. The production cross sections for neutron and proton are 262.69 mb and 1.59 mb by GEMINI++, and 289.25 mb and 1.95 mb by GEMINI, respectively. In the original method, the neutron evaporation is inhibited when the excitation energy is lower than the threshold. However, it is allowed with a certain probability in GEMINI and GEMINI++, where the Hauser-Feshbach evaporation theory is used to predict the evaporation spectra of light particles.

It should be noted that the peaks predicted by the GEMINI++ model for $Z = 23$ and 24 in Fig. 1 are much higher than the calculations by other methods. In order to explore the role of proton evaporation further, the cross sections with respect to proton number are plotted in Fig. 3. The lines for primary and final fragments are coincident due to only neutron evaporation in GRAZING. The tiny differences at $Z = 23$ between these two lines are due to the approximation methods used in calculating the cross section of final fragments in GRAZING. The situation is similar to that of the calculation with GEMINI. Even proton evaporation can be considered in GEMINI, the distributions are not wider than those predicted by GRAZING. For GEMINI++, the evaporated charged particle with the largest cross section of 10.37 mb is α particle. The proton production cross section is 1.59 mb, which is similar with GEMINI. Therefore, it can be inferred that it is the evaporation of α and other particles that causes the large difference between the results from GEMINI and GEMINI++ in Fig. 3. In Ref. [35], it is also mentioned that the TDHF model implemented by GEMINI++ code can reproduce the ^{8}Be decay into two αs. This is due to the improved transmission coefficient in GEMINI++, considering that the evaporation spectra are mainly determined by the transmission coefficients at low energies. In GEMINI++, the transmission coefficients are calculated as the average of transmission coefficients at three different radii considering the thermal fluctuations. While GEMINI does not consider the impact of thermal shape fluctuations or other coupling effects on the Coulomb barrier, and systematically underpredicts the yield of low-energy particles. The radius parameter is obtained from global fitting to the experimental data [67]. The accuracy of prediction for the α particle evaporation at higher energies was studied in Ref. [63].

B. Fission

GRAZING-F theory was developed [49] by implementing the GRAZING model with the classical fission formulas of Vandenbosch and Huizenga [50]. In the following, GEMINI and GEMINI++ will be used to deal with the fission of the primary fragments, and the corresponding result will be compared with that in Ref. [49]. Isotopic production cross sections for $^{238}\mathrm{U} + ^{238}\mathrm{U}$ are displayed in Fig. 4. The experimental data at $E_{\mathrm{lab}} = 1628$ (1.10 V_{B}), 1785 (1.21 V_{B}), and 2059 (1.39 V_{B}) MeV are obtained from Ref. [13], where V_{B} is the Coulomb barrier calculated by the Bass potential [70].

For $^{238}\mathrm{U} + ^{238}\mathrm{U}$, the projectile and the target are identical. In GRAZING, the cross sections of projectilelike fragments are calculated, whereas targetlike fragments are complementary to the former ones. It is assumed that the distributions of excitation energy for the targetlike and projectilelike fragments are the same. Therefore, the cross sections for the final fragments predicted in GRAZING include half of the projectilelike fragments and half of the corresponding targetlike fragments, and the calculated cross sections will be doubled.

From Fig. 4, it can be seen that the cross sections for the final fragments predicted by GRAZING-F, GEMINI, and GEMINI++ models, which consider fission in the deexcitation, are all much lower than those of the primary fragments. With the increasing proton number, theoretical predictions for final fragments are much lower than primary fragments. The predictions of these three models are all too small to be seen for $Z = 100$ at the three energies. It can be seen clearly

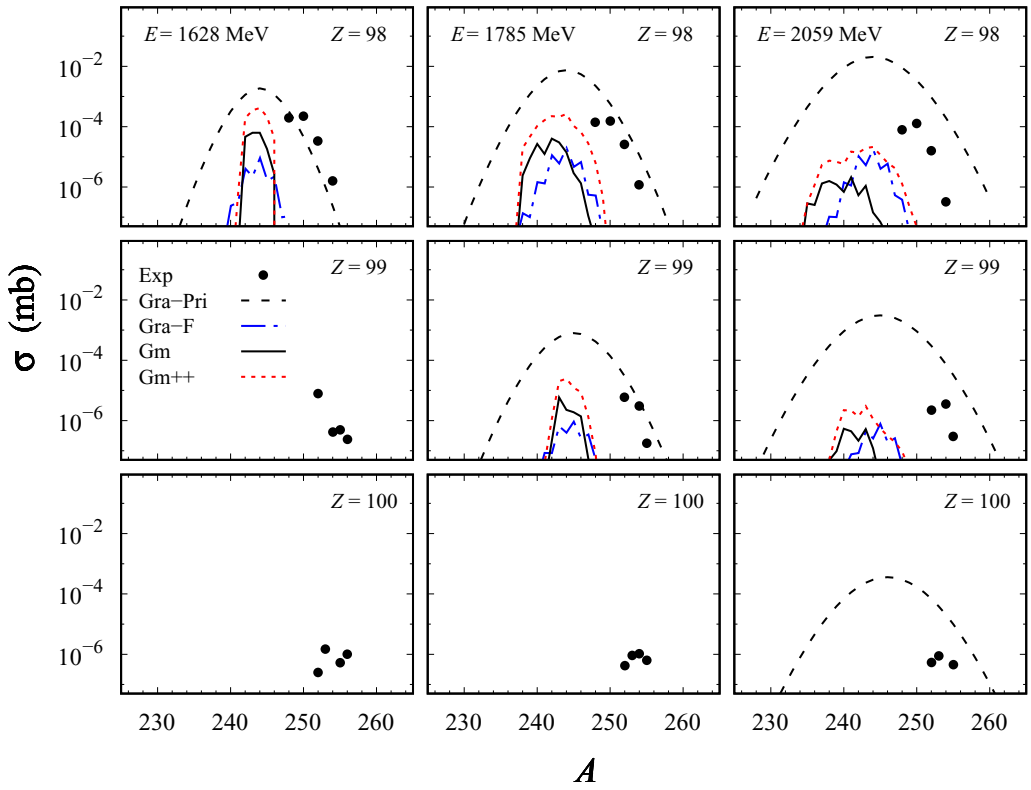

FIG. 4. Targetlike isotopic production cross sections for ^{238}U + ^{238}U at $E_{\rm lab}$ = 1628, 1785, 2059 MeV. The experimental data from Ref. [13] are shown as solid circles. The dashed (Gra-Pri) lines represent the primary fragments predicted by the original GRAZING. The predictions shown as the dash-dotted lines are calculated by GRAZING-F [49]. Final fragments predicted by GRAZING plus GEMINI and GEMINI++ are represented by solid (Gm) and the dotted lines (Gm++), respectively.

that cross section predicted by GEMINI++ are overall higher than GEMINI and GRAZING-F. The predictions of GEMINI are higher than those of GRAZING-F at $E_{\rm lab}$ = 1628 MeV and 1785 MeV, while they are much lower for $Z = 98$ at $E_{\rm lab}$ = 2059 MeV.

The isotopic production cross sections for ^{136}Xe + ^{248}Cm at $E_{\rm lab}$ = 769 MeV (1.03 $V_{\rm B}$) [69] are shown in Fig. 5. The produced heavier fragments are close to the target nucleus with $Z = 96$ and their excitation energies are much smaller than those shown in Fig. 4. Therefore, the reduction degree caused by fission compared to the primary fragments is not obvious and the difference of the cross sections predicted by different models is also not significant. From this figure, it can be seen that the predictions by GEMINI++ and GRAZING-F are very close in the right side of the peak for the six isotopic chains, while results of GEMINI++ are higher than those of GRAZING-F on the left side of the peak, which is due to the strong ability of neutron evaporation considered in GEMINI++. It can also be seen that the predictions by GEMINI are distinctly lower than those by GEMINI++.

Compared with the results shown in Fig. 5, the agreement between theoretical predictions and experimental data shown in Fig. 4 seems poor. The difference between the results shown in the two figures is that the proton numbers of the heavier fragments ($Z = 98, 99, 100$) are far away from the proton number of the target or projectile nuclei ($Z = 92$) in Fig. 4. However, it can be seen from Fig. 4 that the maximum cross sections of each isotope chain predicted by GEMINI++ are very close to the experimental data, and much better than the results predicted by both GEMINI and GRAZING-F, although the mass numbers of the maximum cross sections are inconsistent with the experimental data. One of the main causes of the discrepancy is the diabatic approximation used in GRAZING [19,20], where the transfers are instant and only relative to the projectile or the target, but not to the nuclei with a closer neutron number or proton number. Taking $Z = 98$ as an example, the maximum cross sections predicted by GRAZING will be located at $\Delta Z = +6$ and $\Delta N = 0$ at any energy, which is the isotope ^{244}U in Fig. 4. When more nucleons are transferred, more time is needed for the transfer process. Therefore, the instant transfer approximation used in GRAZING needs to be improved in further studies.

It is important to investigate deeply the difference between the predictions of GEMINI and GEMINI++, considering their extensive applications [33–35,38,51–54]. In Fig. 6, the primary projectilelike and targetlike isotopic production cross sections for ^{136}Xe + ^{248}Cm are displayed. It can be seen that the cross sections for the primary fragments predicted by GRAZING are limited to the very small range. Considering the simple neutron evaporation in the original GRAZING model, we have verified that the isotope cross section will not be changed much. The deexcitations of the targetlike primary

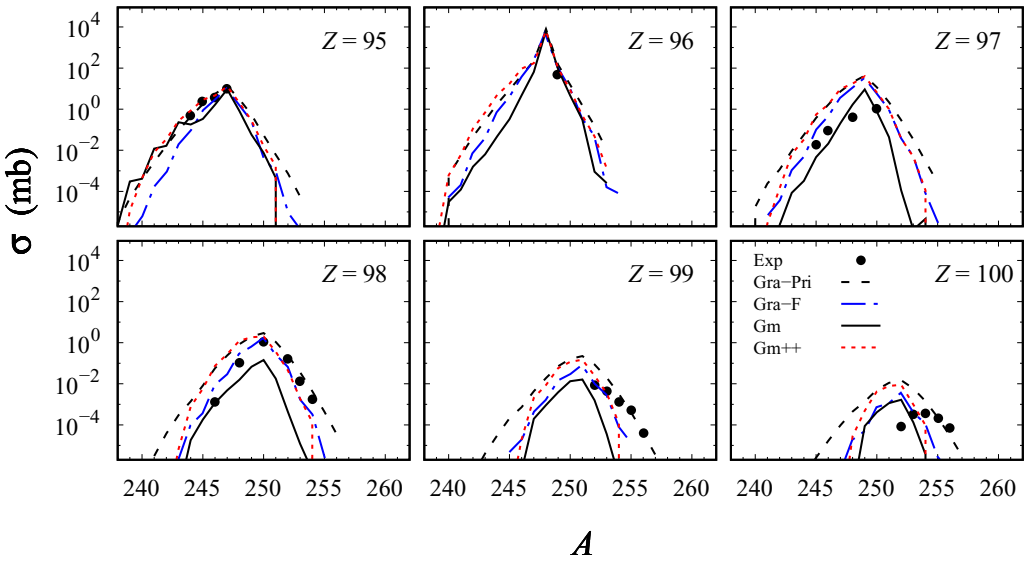

FIG. 5. Same as Fig. 4 but for ^{136}Xe + ^{248}Cm at $E_{\rm lab}$ = 769 MeV. The experimental data are obtained from Ref. [69].

fragments predicted by GEMINI++ and GEMINI are plotted in Figs. 7 and 8, respectively, while the projectilelike fragments are not plotted in order to clarify the role of fission. It can be seen that fission plays a significant role in the final isotope distributions, when implemented with GEMINI++ and GEMINI approach in GRAZING model. Large number of fission fragments can be seen in the medium-heavy nucleus region in Figs. 7 and 8. However, there are significant differences between the predictions in the two figures.

In Fig. 5, the cross sections predicted by GEMINI are obviously smaller than those predicted by GEMINI++ for the case of Z = 98–100. When the isotope cross sections are plotted in the chart of nuclei, apparently wider isotope distributions predicted by GEMINI can be seen than those by GEMINI++. The isotope distributions predicted by GEMINI++ due to fission locate in a certain area in medium-heavy nucleus region, whereas the isotope distributions predicted by GEMINI cover the whole proton number range lighter than the heaviest targetlike fragments. Many new neutron-rich isotopes with Z = 40–82 are predicted by the current GEMINI calculation.

GEMINI generally overpredicts the width of fission fragment mass and charge distributions [67]. This can also be seen in Figs. 7 and 8. This is also the reason why the isotope cross sections generated by GEMINI are overall lower than those by GEMINI++ in Figs. 4 and 5. It was mentioned [67] that it might be due to a failure of the fission model used in GEMINI model. For lighter nuclei, the shape difference between the saddle and scission points is very small during the saddle-to-scission motion. Whereas the neck between two fragments disappears and a deformed mononucleus is formed for very heavy nuclei, the asymmetry degree of freedom cannot be defined anymore. This point was not taken into account in GEMINI where the Moretto formalism [65,67] is used. In

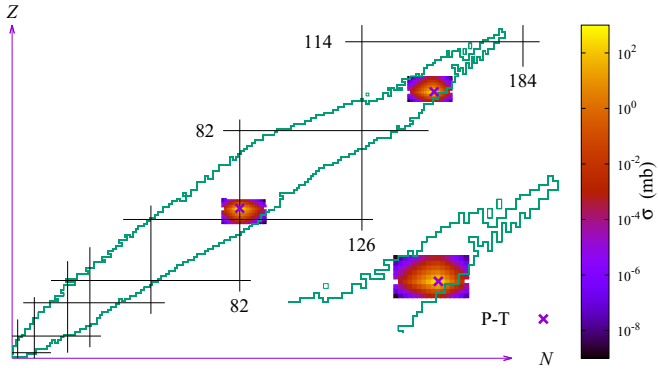

FIG. 6. Primary projectilelike and targetlike isotopic production cross sections of the MNT reaction ^{136}Xe + ^{248}Cm at $E_{\rm lab}$ = 769 MeV, which are calculated with GRAZING model. The black lines represent the assumed positions of corresponding neutron and proton shells. The enlarged targetlike fragment distribution is plotted as the insert located at the bottom right position, which shares the same coordinate systems.

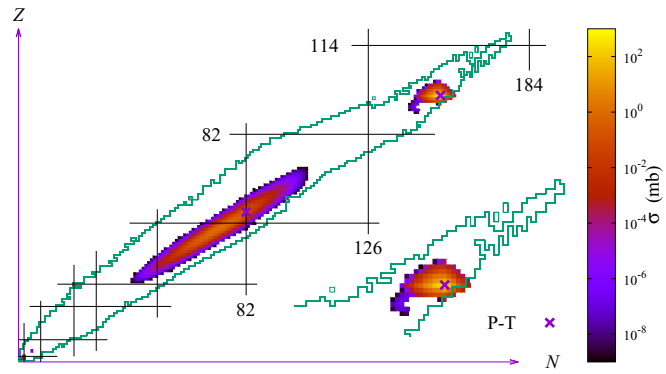

FIG. 7. Same as Fig. 6 but for final targetlike isotopic production cross sections, which are calculated with GRAZING plus GEMINI++ model. The cross symbols denote the locations of the projectile and target.

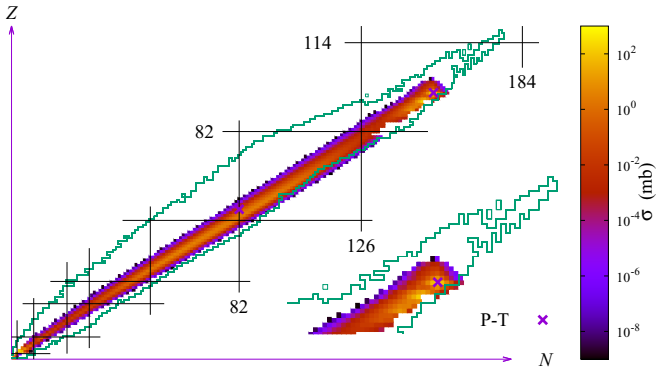

FIG. 8. Same as Fig. 6 but for final targetlike isotopic production cross sections, which are calculated with GRAZING plus GEMINI model.

GEMINI++, more reasonable Bohr-Wheeler formula is used to predict the symmetric fission yield for heavy nuclei.

IV. CONCLUSIONS

In summary, this is the first time to combine the semiclassical GRAZING model and the Monte Carlo statistical model GEMINI, GEMINI++. By doing this, both evaporation and fission processes can be considered in the deexcitation process and the theoretical descriptions for the MNT reactions of heavy and superheavy systems have been significantly improved.

Based on the present calculation, it is found that the results predicted by GEMINI++ reproduce the experimental data better than those by the other two models. For light particle evaporation, the predictions by GEMINI and GEMINI++ significantly improve the results compared with the original method in GRAZING. The important role of charged particle evaporation, especially the impact of α evaporation, is first revealed by GEMINI++ for $^{64}\mathrm{Ni} + {}^{238}\mathrm{U}$ at $E_{\mathrm{c.m.}} = 307.5$ MeV. For the deexcitation of heavier fragments, GEMINI and GEMINI++ perform better than the original method used in GRAZING by considering fission.

However, GEMINI highly overpredicts the fission probability and the width of fission isotope distributions compared with GEMINI++. For fragments far away from the target nucleus in $^{238}\mathrm{U} + {}^{238}\mathrm{U}$, the predictions of GRAZING-F are generally lower than those of GRAZING plus GEMINI++. One of the main reasons for the unsatisfactory situation with the fission for $^{238}\mathrm{U} + {}^{238}\mathrm{U}$ is the unsuitable diabatic approximation used in GRAZING, which needs to be improved in further works.

ACKNOWLEDGMENTS

We thank Dr. Gen Zhang for the instructive comments that greatly improved the manuscript. This work is supported by the National Key R&D Program of China (Contract No. 2018YFA0404404), the National Natural Science Foundation of China (Grants Nos. 11635015, 11805120, 11635003, 11705285, 11805280, 11811530071, U1867212, and U1732145), and the Project funded by China Postdoctoral Science Foundation (Grant Nos. 2017M621035 and 2017M621442).

[1] R. Bass, *Nuclear Reactions with Heavy Ions* (Springer, Berlin, 2010).
[2] L. Corradi, G. Pollarolo, and S. Szilner, J. Phys. G: Nucl. Part. Phys. **36**, 113101 (2009).
[3] C. J. Lin, *Heavy-ion Nuclear Reactions* (Harbin Engineering University Press, Harbin, 2015).
[4] C. H. Dasso, G. Pollarolo, and A. Winther, Phys. Rev. Lett. **73**, 1907 (1994).
[5] G. G. Adamian, N. V. Antonenko, and A. S. Zubov, Phys. Rev. C **71**, 034603 (2005).
[6] R. Broda, J. Phys. G: Nucl. Part. Phys. **32**, R151 (2006).
[7] V. Zagrebaev and W. Greiner, Phys. Rev. Lett. **101**, 122701 (2008).
[8] Z. Q. Feng, G. M. Jin, and J. Q. Li, Phys. Rev. C **80**, 067601 (2009).
[9] G. G. Adamian, N. V. Antonenko, V. V. Sargsyan, and W. Scheid, Phys. Rev. C **81**, 024604 (2010).
[10] G. G. Adamian, N. V. Antonenko, V. V. Sargsyan, and W. Scheid, Phys. Rev. C **81**, 057602 (2010).
[11] V. F. Comas, S. Heinz, S. Hofmann, D. Ackermann, J. A. Heredia, F. P. Heßberger, J. Khuyagbaatar, B. Kindler, B. Lommel, and R. Mann, Eur. Phys. J. A **49**, 112 (2013).
[12] E. M. Kozulin, E. Vardaci, G. N. Knyazheva, A. A. Bogachev, S. N. Dmitriev, I. M. Itkis, M. G. Itkis, A. G. Knyazev, T. A. Loktev, K. V. Novikov, E. A. Razinkov, O. V. Rudakov, S. V. Smirnov, W. Trzaska, and V. I. Zagrebaev, Phys. Rev. C **86**, 044611 (2012).
[13] J. V. Kratz, M. Schädel, and H. W. Gäggeler, Phys. Rev. C **88**, 054615 (2013).
[14] Y. X. Watanabe, Y. H. Kim, S. C. Jeong, Y. Hirayama, N. Imai, H. Ishiyama, H. S. Jung, H. Miyatake, S. Choi, J. S. Song, E. Clement, G. de France, A. Navin, M. Rejmund, C. Schmitt, G. Pollarolo, L. Corradi, E. Fioretto, D. Montanari, M. Niikura, D. Suzuki, H. Nishibata, and J. Takatsu, Phys. Rev. Lett. **115**, 172503 (2015).
[15] J. S. Barrett, W. Loveland, R. Yanez, S. Zhu, A. D. Ayangeakaa, M. P. Carpenter, J. P. Greene, R. V. F. Janssens, T. Lauritsen, E. A. McCutchan, A. A. Sonzogni, C. J. Chiara, J. L. Harker, and W. B. Walters, Phys. Rev. C **91**, 064615 (2015).
[16] A. Vogt, M. Siciliano, B. Birkenbach, P. Reiter, K. Hadyńska-Klęk, C. Wheldon, J. J. Valiente-Dobón, E. Teruya, N. Yoshinaga, K. Arnswald, D. Bazzacco, A. Blazhev, A. Bracco, B. Bruyneel, R. S. Chakrawarthy, R. Chapman, D. Cline, L. Corradi, F. C. L. Crespi, M. Cromaz, G. de Angelis, J. Eberth, P. Fallon, E. Farnea, E. Fioretto, C. Fransen, S. J. Freeman, B. Fu, A. Gadea, W. Gelletly, A. Giaz, A. Görgen, A. Gottardo, A. B. Hayes,

H. Hess, R. Hetzenegger, R. Hirsch, H. Hua, P. R. John, J. Jolie, A. Jungclaus, V. Karayonchev, L. Kaya, W. Korten, I. Y. Lee, S. Leoni, X. Liang, S. Lunardi, A. O. Macchiavelli, R. Menegazzo, D. Mengoni, C. Michelagnoli, T. Mijatović, G. Montagnoli, D. Montanari, C. Müller-Gatermann, D. Napoli, C. J. Pearson, Z. Podolyák, G. Pollarolo, A. Pullia, M. Queiser, F. Recchia, P. H. Regan, J. M. Régis, N. Saed-Samii, E. Şahin, F. Scarlassara, M. Seidlitz, B. Siebeck, G. Sletten, J. F. Smith, P. A. Söderström, A. M. Stefanini, O. Stezowski, S. Szilner, B. Szpak, R. Teng, C. Ur, D. D. Warner, K. Wolf, C. Y. Wu, and K. O. Zell, Phys. Rev. C **96**, 024321 (2017).

[17] E. M. Kozulin, V. I. Zagrebaev, G. N. Knyazheva, I. M. Itkis, K. V. Novikov, M. G. Itkis, S. N. Dmitriev, I. M. Harca, A. E. Bondarchenko, A. V. Karpov, V. V. Saiko, and E. Vardaci, Phys. Rev. C **96**, 064621 (2017).

[18] H. M. Devaraja, S. Heinz, O. Beliuskina, V. Comas, S. Hofmann, C. Hornung, G. Münzenberg, K. Nishio, D. Ackermann, Y. K. Gambhir, M. Gupta, R. A. Henderson, F. P. Heßberger, J. Khuyagbaatar, B. Kindler, B. Lommel, K. J. Moody, J. Maurer, R. Mann, A. G. Popeko, D. A. Shaughnessy, M. A. Stoyer, and A. V. Yeremin, Phys. Lett. B **748**, 199 (2015).

[19] A. Winther, Nucl. Phys. A **572**, 191 (1994).

[20] A. Winther, Nucl. Phys. A **594**, 203 (1995).

[21] L. Corradi, A. M. Stefanini, D. Ackermann, S. Beghini, G. Montagnoli, C. Petrache, F. Scarlassara, C. H. Dasso, G. Pollarolo, and A. Winther, Phys. Rev. C **49**, R2875 (1994).

[22] S. Szilner, L. Corradi, G. Pollarolo, S. Beghini, R. B. Behera, E. Fioretto, A. Gadea, F. Haas, A. Latina, G. Montagnoli, F. Scarlassara, A. M. Stefanini, M. Trotta, A. M. Vinodkumar, and Y. Wu, Phys. Rev. C **71**, 044610 (2005).

[23] L. Zhu, Z. Q. Feng, and F. S. Zhang, J. Phys. G: Nucl. Part. Phys. **42**, 085102 (2015).

[24] L. Zhu, J. Su, and F.-S. Zhang, Phys. Rev. C **93**, 064610 (2016).

[25] L. Zhu, J. Su, W. J. Xie, and F. S. Zhang, Phys. Rev. C **94**, 054606 (2016).

[26] M. H. Mun, G. G. Adamian, N. V. Antonenko, Y. Oh, and Y. Kim, Phys. Rev. C **91**, 054610 (2015).

[27] L. Zhu, P. W. Wen, C. J. Lin, X. J. Bao, J. Su, C. Li, and C. C. Guo, Phys. Rev. C **97**, 044614 (2018).

[28] J. Li, C. Li, P. Wen, and F. S. Zhang, J. Phys.: Conf. Ser. **1014**, 012019 (2018).

[29] V. I. Zagrebaev and W. Greiner, Phys. Rev. C **87**, 034608 (2013).

[30] A. V. Karpov and V. V. Saiko, Phys. Rev. C **96**, 024618 (2017).

[31] C. Simenel, Phys. Rev. Lett. **106**, 112502 (2011).

[32] X. Jiang and S. Yan, Phys. Rev. C **90**, 024612 (2014).

[33] A. S. Umar, V. E. Oberacker, and C. Simenel, Phys. Rev. C **94**, 024605 (2016).

[34] K. Sekizawa, Phys. Rev. C **96**, 041601 (2017).

[35] B. J. Roy, Y. Sawant, P. Patwari, S. Santra, A. Pal, A. Kundu, D. Chattopadhyay, V. Jha, S. K. Pandit, V. V. Parkar, K. Ramachandran, K. Mahata, B. K. Nayak, A. Saxena, S. Kailas, T. N. Nag, R. N. Sahoo, P. P. Singh, and K. Sekizawa, Phys. Rev. C **97**, 034603 (2018).

[36] C. Li, F. Zhang, J. Li, L. Zhu, J. Tian, N. Wang, and F. S. Zhang, Phys. Rev. C **93**, 014618 (2016).

[37] N. Wang and L. Guo, Phys. Lett. B **760**, 236 (2016).

[38] C. Li, P. Wen, J. Li, G. Zhang, B. Li, X. Xu, Z. Liu, S. Zhu, and F. S. Zhang, Phys. Lett. B **776**, 278 (2018).

[39] A. Winther, Fisika **22**, 41 (1990).

[40] G. Pollarolo and A. Winther, Phys. Rev. C **62**, 054611 (2000).

[41] http://personalpages.to.infn.it/∼nanni/grazing/.

[42] G. Pollarolo, Phys. Rev. Lett. **100**, 252701 (2008).

[43] L. Corradi, A. M. Vinodkumar, A. M. Stefanini, E. Fioretto, G. Prete, S. Beghini, G. Montagnoli, F. Scarlassara, G. Pollarolo, F. Cerutti, and A. Winther, Phys. Rev. C **66**, 024606 (2002).

[44] A. Vogt, B. Birkenbach, P. Reiter, L. Corradi, T. Mijatović, D. Montanari, S. Szilner, D. Bazzacco, M. Bowry, A. Bracco, B. Bruyneel, F. C. L. Crespi, G. de Angelis, P. Désesquelles, J. Eberth, E. Farnea, E. Fioretto, A. Gadea, K. Geibel, A. Gengelbach, A. Giaz, A. Görgen, A. Gottardo, J. Grebosz, H. Hess, P. R. John, J. Jolie, D. S. Judson, A. Jungclaus, W. Korten, S. Leoni, S. Lunardi, R. Menegazzo, D. Mengoni, C. Michelagnoli, G. Montagnoli, D. Napoli, L. Pellegri, G. Pollarolo, A. Pullia, B. Quintana, F. Radeck, F. Recchia, D. Rosso, E. Sahin, M. D. Salsac, F. Scarlassara, P. A. Söderström, A. M. Stefanini, T. Steinbach, O. Stezowski, B. Szpak, C. Theisen, C. Ur, J. J. Valiente-Dobón, V. Vandone, and A. Wiens, Phys. Rev. C **92**, 024619 (2015).

[45] E. Vigezzi and A. Winther, Ann. Phys. (NY) **192**, 432 (1989).

[46] D. Montanari, L. Corradi, S. Szilner, G. Pollarolo, E. Fioretto, G. Montagnoli, F. Scarlassara, A. M. Stefanini, S. Courtin, A. Goasduff, F. Haas, D. Jelavić Malenica, C. Michelagnoli, T. Mijatović, N. Soić, C. A. Ur, and M. Varga Pajtler, Phys. Rev. Lett. **113**, 052501 (2014).

[47] P. W. Wen, C. Li, L. Zhu, C. J. Lin, and F. S. Zhang, J. Phys. G: Nucl. Part. Phys. **44**, 115101 (2017).

[48] R. Yanez and W. Loveland, GRAZING-F, http://grazingf.oregonstate.edu/.

[49] R. Yanez and W. Loveland, Phys. Rev. C **91**, 044608 (2015).

[50] R. Vandenbosch and J. Huizenga, *Nuclear Fission* (Academic Press, New York, 1973).

[51] P. Marini, H. Zheng, M. Boisjoli, G. Verde, A. Chbihi, P. Napolitani, G. Ademard, L. Augey, C. Bhattacharya, B. Borderie, R. Bougault, J. D. Frankland, Q. Fable, E. Galichet, D. Gruyer, S. Kundu, M. La Commara, I. Lombardo, O. Lopez, G. Mukherjee, M. Parlog, M. F. Rivet, E. Rosato, R. Roy, G. Spadaccini, M. Vigilante, P. C. Wigg, and A. Bonasera, Phys. Lett. B **756**, 194 (2016).

[52] F. Zhang, C. Li, P. W. Wen, H. Liu, and F. S. Zhang, Eur. Phys. J. A **52**, 281 (2016).

[53] L. Zhu, J. Su, W. J. Xie, and F. S. Zhang, Phys. Lett. B **767**, 437 (2017).

[54] J. Su, L. Zhu, and C. C. Guo, Phys. Lett. B **782**, 682 (2018).

[55] R. J. Charity, Phys. Rev. C **82**, 014610 (2010).

[56] D. Mancusi, R. J. Charity, and J. Cugnon, Phys. Rev. C **82**, 044610 (2010).

[57] R. Broglia and A. Winther, *Heavy Ion Reactions: The Elementary Processes* (Addison-Wesley, Boston, 1991).

[58] K. Dietrich and K. Hara, Nucl. Phys. A **211**, 349 (1973).

[59] J. M. Quesada, G. Pollarolo, R. A. Broglia, and A. Winther, Nucl. Phys. A **442**, 381 (1985).

[60] J. H. Sørensen and A. Winther, J. Phys. G: Nucl. Part. Phys. **17**, 341 (1991).

[61] R. A. Broglia, R. A. Ricci, C. H. Dasso, and S. I. D. Fisica, *Nuclear Structure and Heavy-ion Collisions: Varenna on Lake Como, Villa Monastero, 9th-21st July 1979* (North-Holland, Italy, 1981).

[62] R. J. Charity, M. A. McMahan, G. J. Wozniak, R. J. McDonald, L. G. Moretto, D. G. Sarantites, L. G. Sobotka, G. Guarino,

A. Pantaleo, L. Fiore, A. Gobbi, and K. D. Hildenbrand, Nucl. Phys. A **483**, 371 (1988).
[63] D. Mancusi, J. Cugnon, A. Boudard, S. Leray, and R. Charity, in *Proceedings to the Satellite Meeting on Nuclear Spallation Reactions, International Topical Meeting on Nuclear Research Applications and Utilization of Accelerators 2009* (International Atomic Energy Agency (IAEA), Vienna, 2009).
[64] B. Blank, G. Canchel, F. Seis, and P. Delahaye, Nucl. Instrum. Methods Phys. Res., Sect. B **416**, 41 (2018).
[65] L. G. Moretto and J. S. Sventek, Phys. Lett. B **58**, 26 (1975).
[66] N. Bohr and J. A. Wheeler, Phys. Rev. **56**, 426 (1939).
[67] R. Charity, in *Joint ICTP-IAEA Advanced Workshop on Model Codes for Spallation Reactions, IAEA*, Trieste, Italy (International Atomic Energy Agency (IAEA), Vienna, 2008), p. 139.
[68] L. Corradi, A. M. Stefanini, C. J. Lin, S. Beghini, G. Montagnoli, F. Scarlassara, G. Pollarolo, and A. Winther, Phys. Rev. C **59**, 261 (1999).
[69] R. B. Welch, K. J. Moody, K. E. Gregorich, D. Lee, and G. T. Seaborg, Phys. Rev. C **35**, 204 (1987).
[70] R. Bass, Nucl. Phys. A **231**, 45 (1974).